*Polymers* **2014**, *6*, 686-705; doi:10.3390/polym6030686

OPEN ACCESS

*polymers*

**ISSN 2073-4360**

www.mdpi.com/journal/polymers

*Article*

# All Green Composites from Fully Renewable Biopolymers: Chitosan-Starch Reinforced with Keratin from Feathers

**Cynthia G. Flores-Hernández [1,3], Arturo Colín-Cruz [1], Carlos Velasco-Santos [2,3], Víctor M. Castaño [3,7], José L. Rivera-Armenta [4], Armando Almendarez-Camarillo [5], Perla E. García-Casillas [6] and Ana L. Martínez-Hernández [2,3,*]**

1 Department of Environmental Science, Chemistry Faculty, Autonomous University of Mexico State, Esq Paseo Colón and Paseo Tollocan, Col. Residencial Colón 50180 Toluca, Estado de Mexico, Mexico; E-Mails: cynthiagraciela@hotmail.com (C.G.F.-H.); acolinc@uaemex.mx (A.C.-C.)

2 Division of Postgraduate Studies and Research, Technological Institute of Querétaro, Av. Tecnológico s/n, esq Gral. Mariano Escobedo, Col. Centro Histórico, C.P. 76000, Santiago de Querétaro, Querétaro, Mexico; E-Mail: cylaura@gmail.com

3 Department of Molecular Materials Engineering, Centre of Applied Physics and Advanced Technology, National Autonomous University of Mexico, Boulevard Juriquilla No. 3001, C.P. 76230, Juriquilla, Santiago de Queretaro, Mexico; E-Mail: victor.m.castano@gmail.com

4 Division of Postgraduate Studies and Research, Technological Institute of Madero City, Juventino Rosas y Jesús Urueta s/n, Col. Los Mangos, C.P. 89440, Ciudad Madero, Tamaulipas, Mexico; E-Mail: jlriveraarmenta@itcm.edu.mx

5 Department of Chemical Engineering, Technological Institute of Celaya, Av. Tecnológico y Antonio García Cubas s/n, Col. Fovissste, C.P. 38010. Celaya, Guanajuato, Mexico; E-Mail: armando@iqcelaya.itc.mx

6 Institute of Engineering and Technology, Autonomous University of Juárez City, Av Del Charro 450 Norte, Col. Partido Romero, C.P. 32310, Ciudad Juarez, Chihuahua, Mexico; E-Mail: pegarcia@uacj.mx

7 Center of Advanced Technology -CIATEQ, Av. El Retablo 150, Col. Constituyentes Fovissste, C.P. 76150, Santiago de Querétaro, Querétaro, Mexico

* Author to whom correspondence should be addressed; E-Mail: almh72@gmail.com; Tel.: +52-442-238-1145; Fax: +52-442-238-1160.

*Received: 30 January 2014; in revised form: 1 March 2014 / Accepted: 4 March 2014 / Published: 11 March 2014*

**Abstract:** The performance as reinforcement of a fibrillar protein such as feather keratin fiber over a biopolymeric matrix composed of polysaccharides was evaluated in this paper. Three different kinds of keratin reinforcement were used: short and long biofibers and rachis particles. These were added separately at 5, 10, 15 and 20 wt% to the chitosan-starch matrix and the composites were processed by a casting/solvent evaporation method. The morphological characteristics, mechanical and thermal properties of the matrix and composites were studied by scanning electron microscopy, thermogravimetric analysis, differential scanning calorimetry and dynamic mechanical analysis. The thermal results indicated that the addition of keratin enhanced the thermal stability of the composites compared to pure matrix. This was corroborated with dynamic mechanical analysis as the results revealed that the storage modulus of the composites increased with respect to the pure matrix. The morphology, evaluated by scanning electron microscopy, indicated a uniform dispersion of keratin in the chitosan-starch matrix as a result of good compatibility between these biopolymers, also corroborated by FTIR. These results demonstrate that chicken feathers can be useful to obtain novel keratin reinforcements and develop new green composites providing better properties, than the original biopolymer matrix.

**Keywords:** keratin; chicken feather; biofibers; chitosan; starch; biopolymer composite

## 1. Introduction

Important efforts to protect the environment are focused on finding alternatives to replace synthetic materials, with a growing array of natural materials. The number of research works aiming to develop polymers or composites with natural materials is constantly increasing; one way to accomplish this is by combining the properties of different materials taking advantage of the biopolymer's characteristics [1–3].

The development of new materials using natural fibers has become an area of great interest, mainly due to the importance of improved materials that can be used in everyday life. Thus, polymers reinforced with natural fibers, have attracted attention among scientists in recent years, due to the need for developing friendly environmental materials that could replace, totally or partially, the currently used materials.

Thus, around the world many scientists have focused their research on using materials from nature. Specifically in the case of composites and films, the use of biopolymers has emerged as an interesting alternative. A clear example is the use of cellulose obtained from plants that has been investigated for several decades [4]. Tang *et al.*, [5] distinguished two kinds of biopolymers: those that come from living organisms and those which need to be polymerized but come from renewable resources and are biodegradable. Taking into account this classification, the first group includes polysaccharide (chitosan, starch, cellulose, among others) and protein (gelatin, collagen, keratin, *etc*.); the second one is well represented by polylactic acid. In this article three biopolymers from the first group have been

combined synergically for the first time to obtain a green composite: chitosan-starch as matrix and keratin biofibers as reinforcement.

Chitosan is composed of β-(1,4)-2-amino-2-deoxy-D-glucose, a deacetylated product of chitin obtained from crustacean wastes. Chitosan has been extensively studied due to its biocompatibility and biodegradability and because of that, it has been used in biomedical and cosmetic applications. In addition this renewable biopolymer has important potential as a packaging polymer due to its ability to form films. Recently several developments involving chitosan and nanostructures were published [6–8], increasing the potential applications of this polysaccharide.

On the other hand, starch has been studied for several decades due to its availability, biodegradability and lower cost. Starch is composed of linear amylose and branched amylopectin, and is considered the main form of stored carbohydrates in plants such as rice, potatoes or corn. Starch can show a thermoplastic behavior if water, glycerol or sorbitol is added as plasticizer. In spite of its many advantages, starch based materials have severe disadvantages due to poor processability, weak mechanical properties, poor long-term stability and high water sensitivity [5,9].

These polysaccharides have been studied combined with synthetic or natural polymers: starch-polyethylene [10], starch-henequen and starch-coconut [11], starch-poly(lactic acid), polyhydroxyester ether, or poly(hydroxybutyrate-co-valerate) [12], poly(vinyl alcohol)-chitosan [13], chitosan-poly(lactic acid) [14] as well as starch-chitosan [6,15,16].

The third biopolymer involved in this research is keratin, a fibrillar protein, found in hair, nails, horn, wool and feathers. Human hair and wool have been amply studied due to textile and medical importance; however feather keratin has not been fully exploited. The basic structure of chicken feathers is composed of a main shaft called rachis, side branches known as barbs and extending from them the barbules. Feather keratin is distinguished by a hierarchical structure, with a highly ordered conformation, the product of large birds' evolution, in fact it is considered as a biological fiber-reinforced composite consisting of a high modulus fiber and a lower modulus viscoelastic matrix. Keratin fibers from feathers are non-abrasive, eco-friendly, biodegradable, renewable, insoluble in organic solvents, and also have good mechanical properties, low density, hydrophobic behavior, ability to dampen sound, warmth retention and finally low cost. These characteristics make keratin fibers from chicken feathers a suitable material to be used as a high structural reinforcement in polymer composites [1,17,18].

During the last decade, an increasing amount of research has been published involving keratin fibers from chicken feather with synthetic polymers, such as grafting with polymethylmethacrylate [19,20] and polyhydroxyethylmethacrylate [21]; composites with polyethylene [22,23], polypropylene [24–26], polymethylmethacrylate [27], polyurethane [28] and phenol-formaldehyde [29], among others [18], however there are only few related to keratin fibers and biopolymers [30,31].

In this paper, the main goal is focused on taking advantage of keratin from chicken feathers, exploiting their properties as a reinforcement in order to develop new green composites with a natural polymer matrix. They are also characterized to observe their morphological structure, thermal and mechanical behavior. Therefore the biopolymers have been studied as an available alternative, with the outstanding advantage of sustainable and environmental friendly character.

## 2. Experimental Section

### *2.1. Materials*

Chitosan (85% deacetylated) was obtained from Sigma Aldrich. Potato starch was purchased from National Starch, Co. (Hammond, IN, USA). Sorbitol was acquired from Golden Bell Reactivos, acetic acid was obtained from J.T. Baker and chicken feathers were supplied by Pilgrim's Pride Company (Querétaro, México).

### *2.2. Preparation of Keratin Biofibers and Ground Rachis*

Feathers, as obtained from Pilgrims´s Pride, were washed with water and ethanol and dried in order to be clean white, sanitized and odor free. Then keratin biofibers were obtained according to a patented process by Schmidt [32], these are called long biofibers (LB). On the other hand, short biofibers and ground rachis were prepared by cutting manually barbs and barbules (SB) from quill (GQ); once separated, each raw material was finely ground in a hammer mill (Pulvex, model 200, sieve 4 mm).

### *2.3. Composite Preparation*

Chitosan solution was prepared by dispersing 0.2 g of chitosan in 100 mL of acetic acid solution (1%, v/v) and stirred. On the other hand, potato starch solution was prepared by mixing 3.8 g of starch in 100 mL of water and adding sorbitol as a plasticizer (1%, v/v), this solution was heated beyond its gelatinization point (90 °C) for 10 minutes, after it was stirred and cooled to 25 °C [15]. A series of chitosan-starch composite films were prepared by mixing 100 mL of chitosan solution with 100 mL of starch solution (5:95 chitosan:starch). Short and long keratin biofibers and ground rachis were added at 5%, 10%, 15% and 20% (w/w). The mixture was stirred for 20 minutes at room temperature. The resulting mixture was poured into poly(tetrafluoro ethylene) dishes to finish gel formation and later it was cooled at room temperature. Table 1 shows the corresponding concentrations and nomenclature used in the synthesis and characterization of composites.

**Table 1.** Composition and nomenclature of chitosan-starch/keratin reinforced composites.

| Percentage of Keratin Reinforcement (wt%) | Type of Keratin Reinforcement | | |
|---|---|---|---|
| | **Long Biofiber** | **Short Biofiber** | **Ground Quill** |
| 5 | ChS-LB05 | ChS-SB05 | ChS-GQ05 |
| 10 | ChS-LB10 | ChS-SB10 | ChS-GQ10 |
| 15 | ChS-LB15 | ChS-SB15 | ChS-GQ15 |
| 20 | ChS-LB20 | ChS-SB20 | ChS-GQ20 |

### *2.4. Characterization Methods*

Thermogravimetric analyses (TGA) were carried out by TA Instruments SDT 2960 under a nitrogen atmosphere and covering 30–600 °C by a heat rate of 5 °C/min. Dynamical-mechanical analysis (DMA) was performed on a TA Instruments DMA 2980 equipment, operating in dual cantilever bending mode at 1 Hz in frequency, the samples were tested between 30–300 °C.

Differential scanning calorimetry (DSC) was conducted in a TA Instruments model Q200, samples were heated at a rate of 10 °C/min from 15–400 °C. Two samples of each composite were analyzed for thermal and thermomechanical characterization. The morphology of the composites was observed by scanning electron microscopy (SEM) using a JSM-6060LV JEOL microscope at an accelerating voltage of 20 kV. Samples of all composites were fractured using an Adamel Lhomargy DY.22 universal testing machine, to observe by SEM the behavior of the reinforcement and matrix. Fractured samples were mounted on metal stubs and were vacuum-coated with gold at $7 \times 10^{-2}$ mB using argon in a sputter coater EMS 550. The Fourier transform infrared (FTIR) spectra of the films were recorded using an attenuated total refraction (ATR) method in a FTIR spectrometer (Bruker, Tensor 37) with a spectral resolution of 0.6 $cm^{-1}$ and 32 scans in the range of 4000–400 $cm^{-1}$.

## 3. Results and Discussion

### *3.1. Fiber Dispersion and Physical Appearance of Composites*

Composites reinforced with short biofibers are shown in Figure 1; it is possible to see that the biofibers are well dispersed, since they do not show agglomerates or separated phases, and the biofibers are contained in the entire matrix, this is apparent by the homogenous distribution. In addition the appropriate integration of chitosan and starch is demonstrated by a uniform color in the matrix. Figure 2 shows the composites reinforced with ground rachis; it is possible to observe also that in these composites a good distribution of reinforcement was achieved. In both cases the suitable dispersion is due to the polysaccharide matrix and keratin which has a high degree of compatibility, besides the size of the reinforcements enables good embedding without fiber entanglements or rachis agglomerates.

In contrast, long biofiber composites, shown in Figure 3, exhibited a saturation appearance and fiber cumuli are more evident as the reinforcement percentage increases, mainly due to the length of the fiber which is not conducive to being completely wetted by the matrix.

**Figure 1.** Physical appearance of chitosan-starch/short keratin biofiber (ChS-SB) composites, (**a**) 5% of reinforcement, ChS-SB05; (**b**) 10% of reinforcement, ChS-SB10; (**c**) 15% reinforcement ChS-SB15 and (**d**) 20% reinforcement ChS-SB20.

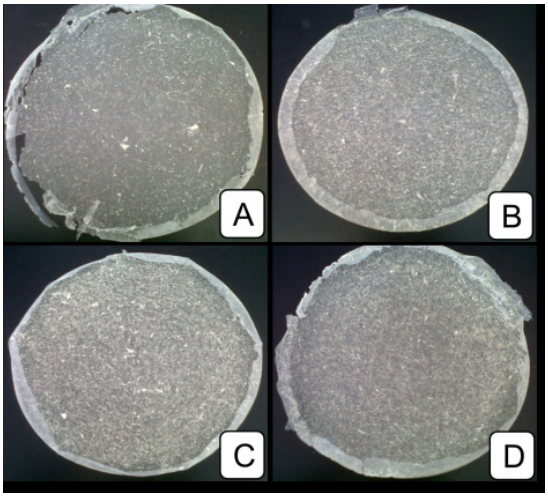

**Figure 2.** Physical appearance of chitosan-starch/grinded quill (ChS-GQ) composites, (**a**) 5% of reinforcement, ChS-GQ05; (**b**) 10% of reinforcement, ChS-GQ10; (**c**) 15% reinforcement ChS-GQ15 and (**d**) 20% reinforcement ChS-GQ20.

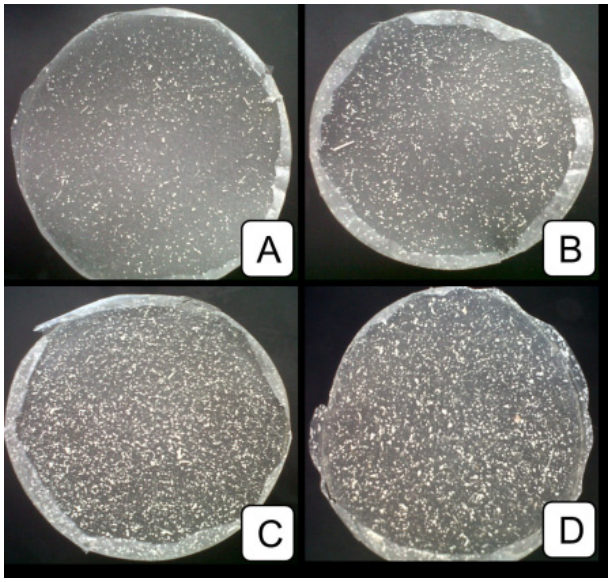


**Figure 3.** Physical appearance of chitosan-starch/long keratin biofiber (ChS-LB) composites, (**a**) 5% of reinforcement, ChS-LB05; (**b**) 10% of reinforcement, ChS-LB10; (**c**) 15% reinforcement ChS-LB15 and (**d**) 20% reinforcement ChS-LB20.

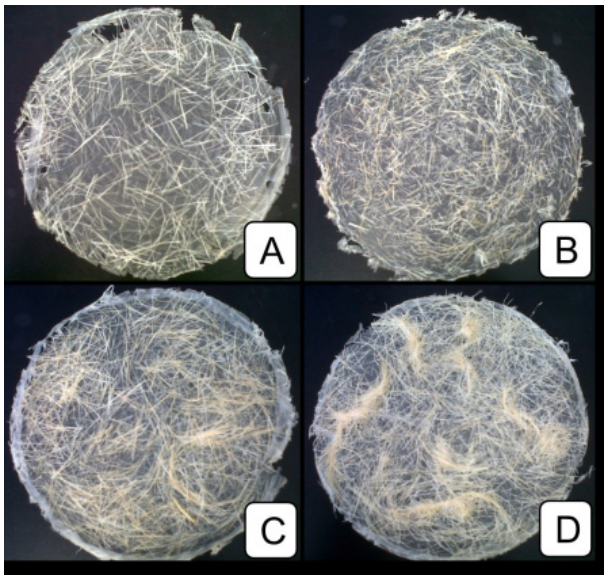


*3.2. Morphology of Composites Studied by Scanning Electron Microscopy*

Surface morphology of chitosan-starch/keratin reinforced composites was studied by SEM. Micrographs of fractured surfaces of ChS-SB05 composite are shown in Figure 4; here it is possible to observe that short fibers and polysaccharides have an appreciable interaction, since matrix is adhered to the fiber surface. Also, the matrix appears with striations and deformations around the fiber; this is evidence of the strength transmitted between fiber and matrix. In addition some fibers' extremities are cracked very close to the matrix, showing good adherence [22,27]. Only a few voids are located in the

surface caused by slips of fibers, but in general good dispersion and evident fiber-polymer interactions were noticed.

**Figure 4.** Scanning electron microscopy (SEM) micrographs of fractured surfaces of chitosan-starch composites reinforced with 5% of short keratin fiber (ChS-SB05).

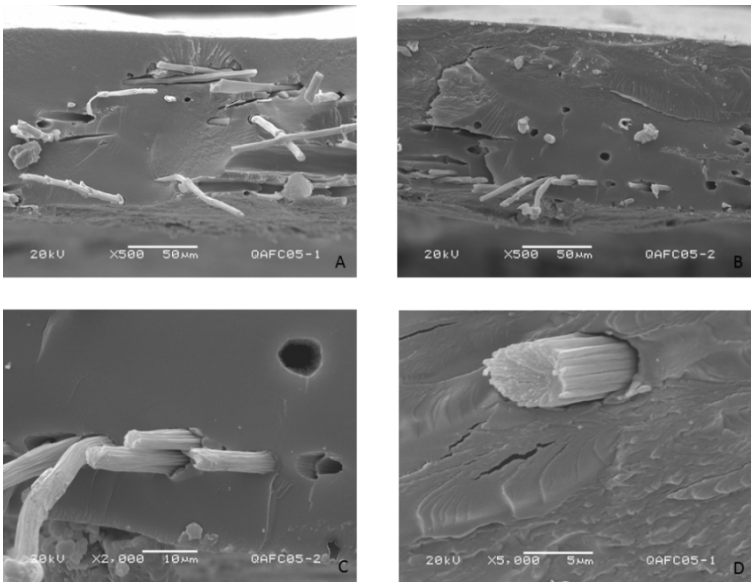


Figure 5 shows SEM images of ChS-LB05 composites, these micrographs reveal the presence of zones with a high quantity of fibers, the majority appear oriented to the load direction. In contrast to the above composite, long fibers are close together and they are not well dispersed, forming bundles that could cause certain weak sites. In spite of these bundles, some fibers play an important role in supporting load, as is evidenced by the fracture of single fibers close to the surface of the matrix.

**Figure 5.** SEM micrographs of fractured surfaces of chitosan-starch composites reinforced with 5% of long keratin fibers (ChS-LB05).

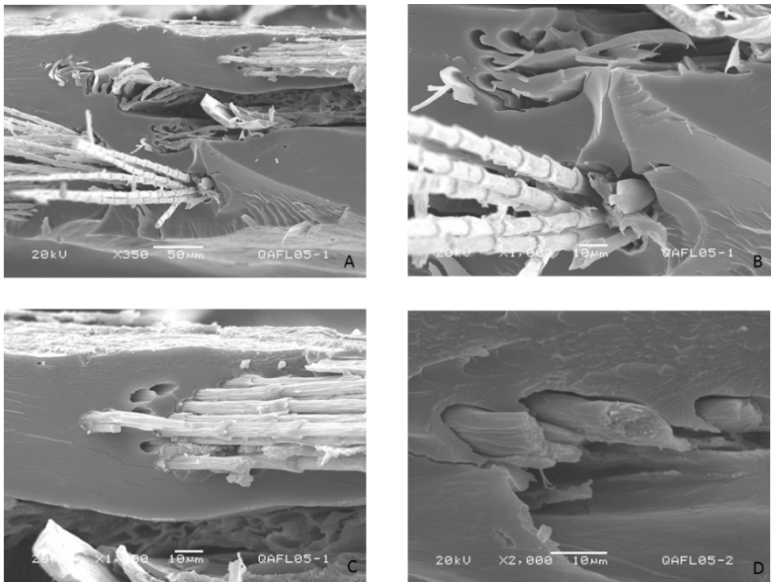

Ground quill particles are very compatible with the matrix, as is demonstrated in Figure 6. These micrographs correspond to ChS-GQ05 composite. The images show good reinforcement dispersion, without appreciable voids, since no shift is observed. Quill is totally disrupted as a result of the load applied, and therefore an adequate interface is presumed.

**Figure 6.** SEM micrographs of fractured surfaces of chitosan-starch composites reinforced with 5% of ground quill reinforcement (ChS-GQ05).

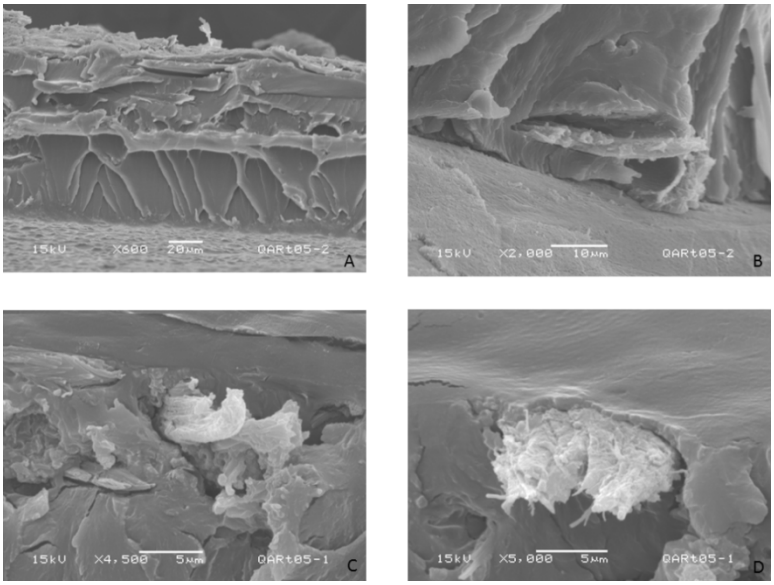


*3.3. Thermogravimetrical Analysis*

TGA results of chitosan-starch/short keratin biofiber (ChS-SB) composites are shown in Figure 7. The thermal behavior observed for these composites can be described in three main steps: the first mass loss (7%) from 30–135 °C is due to the loss of bound-water. The second step is from 220–360 °C, with mass decreasing from 8%–76%, this is associated with a complex process that includes dehydration of the saccharide rings, depolymerization and decomposition of the chitosan units [15,33]. The third step occurred from 450–600 °C with the greatest weight loss corresponding to complete degradation of the polymer [6,15,33]. The thermal behavior of the composites does not change significantly when keratin biofibers are included as reinforcement, the behavior of the thermal decomposition remains almost unaltered for all the composites when compared to the chitosan-starch curve (ChS). It can be seen that the composite with 5% of keratin reinforcement has the highest weight loss (96.6%) and in contrast the composite with 15% shows the lowest weight loss (84.5%); however this effect is related to the inherent variations of natural materials and not to the percentages shown. The TGA curve for short keratin biofiber has a typical performance for keratinous materials: a first loss from 25 °C to around 55 °C due to loss of water, after the process corresponding to denaturation of the helix structure, as well as thermal pyrolysis of the chain linkages, peptide bridges and main skeletal degradation [17,34].

**Figure 7.** Thermogravimetric analysis (TGA) curves for composites chitosan-starch/short keratin biofiber (ChS-SB), with 5%–20% of biofiber included.

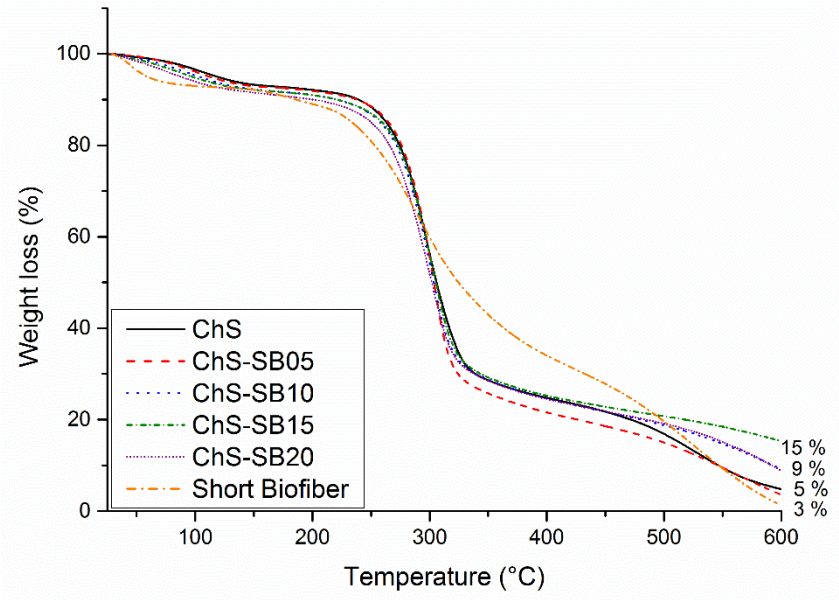


Figure 8 shows TGA diagrams for the composites reinforced with long keratin biofibers (ChS-LB). As is observed, the behavior of these thermogravimetric curves is very similar to the above composites reinforced with short keratin biofibers. Basically the difference is observed in the third stage of decomposition (around 450–600 °C), where all the composites are benefited by keratin presence, since at 600 °C the highest loss mass is for matrix. In addition in the range from 325–475 °C, both 10% and 20% of reinforcement show better stability than that shown by matrix, with 5% and 15% of reinforced composites. Again typical behavior is observed for long keratin biofibers.

**Figure 8.** TGA curves for composites chitosan-starch/long keratin biofiber (ChS-LB), with 5%–20% of biofiber included.

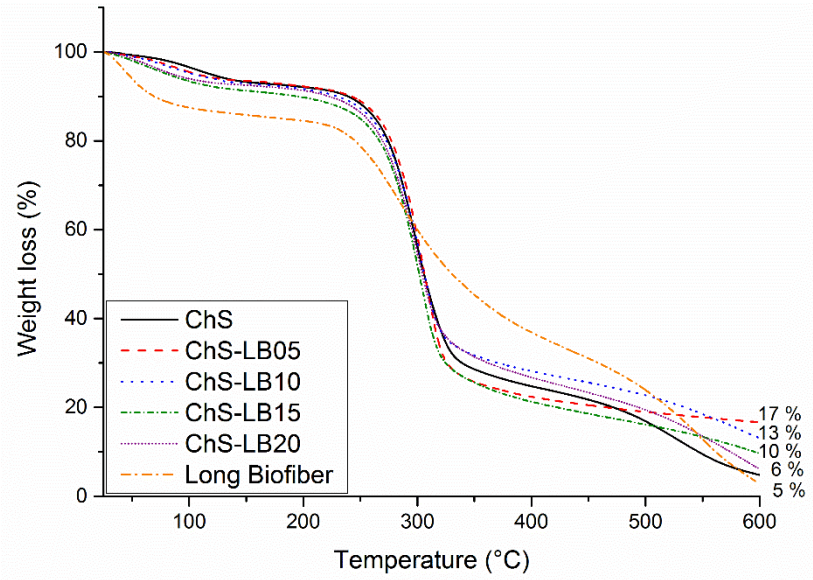

TGA curves of the composites chitosan-starch/ground quill (ChS-GQ) are shown in Figure 9. The initial weight loss (7%) occurs from 40–150 °C and is caused by evaporation of water, while the second range (200–360 °C) with a weight loss of 10%–75% corresponds to a complex process including the dehydration of the saccharide rings, depolymerization, and decomposition of acetylated and deacetylated units of chitosan [6,15,33]. Also, this stage is associated with the destruction of disulfide bonds and the elimination of $H_2S$ originating from amino acid cysteine in keratin [17,34].

It is possible to observe that ground quill slightly improved the thermal behavior of composites, since the weight loss decreased as reinforcement was increased, thus the material with the least weight loss is the composite with 20% of quill reinforcement.

**Figure 9.** TGA curves for composites chitosan-starch/grinded quill (ChS-GQ), with 5%–20% of biofiber included.

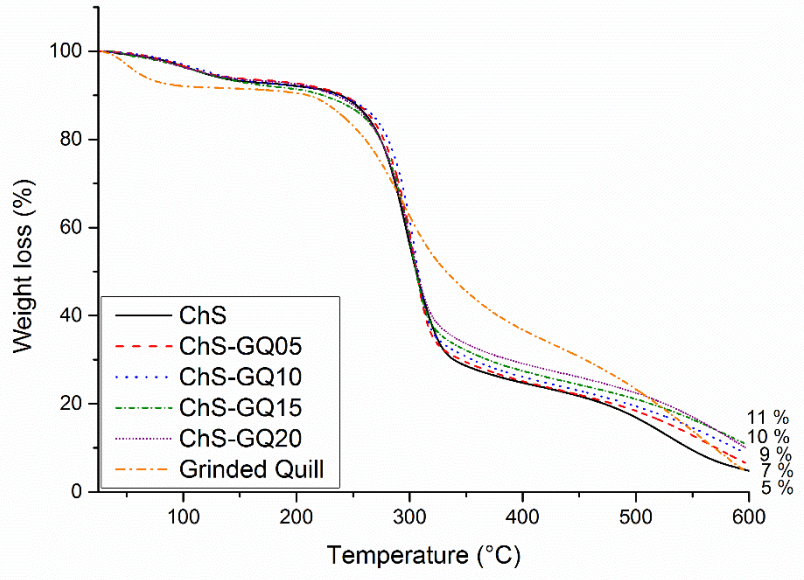


*3.4. Differential Scanning Calorimetry*

Figure 10 shows DSC curves for ChS-SB composites. The endothermic peak around 80–96 °C in the first run corresponds to the evaporation of water and appeared in all the composite samples [15]. The next endothermic peak around 200 °C can be assigned to the crystalline melting temperature found in keratin [35]. The peak at 300 °C is related to keratin, specifically with the destruction of disulfide bonds and the denaturation of the helix structure [17]. Also it could be ascribed to total biopolymer decomposition [15,33]. These results show a decomposition temperature for ChS-SB composites around 290–330 °C, a temperature range that agrees with the highest weight loss observed in TGA.

**Figure 10.** Differential scanning calorimetry (DSC) curves for composites (ChS-SB), with 5%–20% of biofiber included.

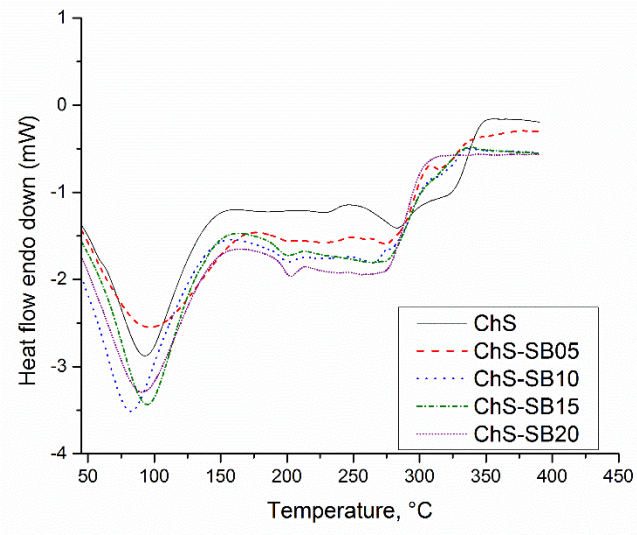


DSC results for ChS-LB composites are shown in Figure 11. These curves show a similar behavior with respect to ChS-SB composites. The initial endothermic peak is approximately at 90–100 °C, associated with loss of water. The second range, around 200 °C, corresponds to the crystalline melting temperature of keratin, whereas the third range from 290–330 °C can be assigned to thermal changes in chitosan, such as dehydration of saccharide rings, decomposition of acetylated and deacetylated units, and also to thermal degradation of keratin with disruption of disulfide bonds and denaturation of helical structures [15,17,33].

**Figure 11.** DSC curves for composites (ChS-LB), with 5%–20% of biofiber included.

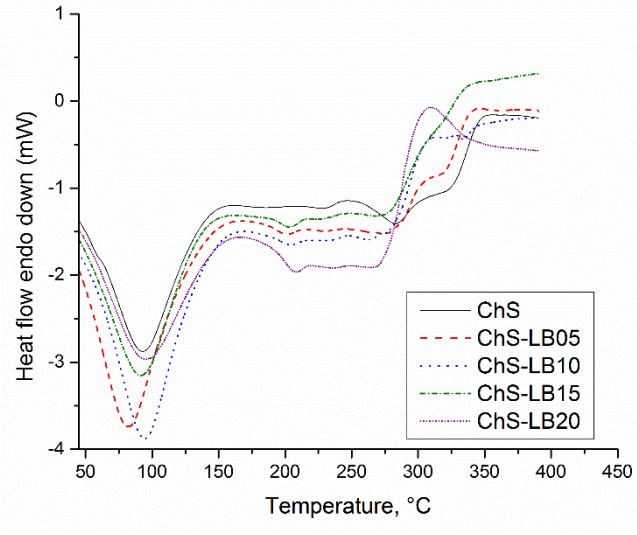


The results of DSC for ChS-GQ composites are summarized in Figure 12. The peaks are very similar for this Figure and Figures 10 and 11, and can be assigned to the mentioned thermal changes in chitosan, starch and keratin.

As is observed for all composite DSC curves, thermal behavior is affected by keratin fibers and quill presence, since keratin undergoes different reactions caused by the thermally sensitive behavior of amino acids.

**Figure 12.** DSC curves for composites (ChS-GQ), with 5%–20% of quill included.

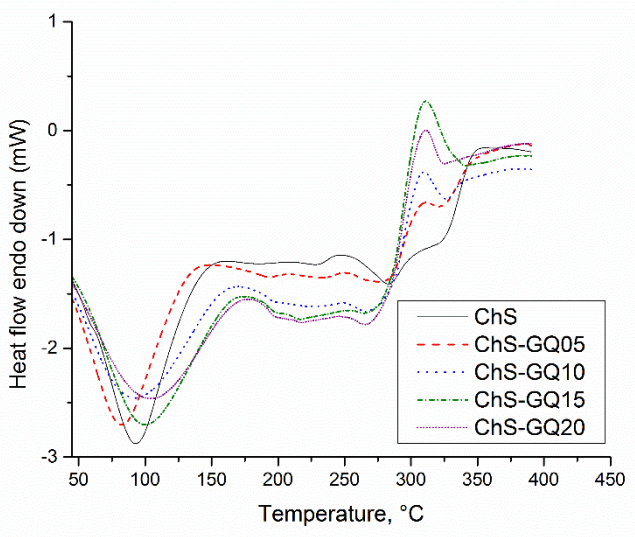


*3.5. Dynamical Mechanical Analysis*

The viscoelastic behavior of composites is studied by dynamical mechanical analysis, obtaining a complex modulus ($E^*$), formed by a storage modulus ($E'$) which represents solid-like (elastic) response and loss modulus ($E''$) related to the liquid-like (viscous flow) characteristic. Taking into account this definition, Brostow *et al.* linked the concept of brittleness to the storage modulus, and according to their affirmation a material with high $E'$ will not be brittle [36,37]. Therefore as is observed in the following results keratin reinforcement decreases brittleness in composites, since for all composites $E'$ is higher than the value for the biopolymeric matrix.

The storage modulus ($E'$) for the ChS-SB composites is depicted in Figure 13. As can be observed, the composite with 5% of reinforcement shows an increased value for $E'$ at 35 °C, reaching 1142 MPa, which means a 763% higher value than the biopolymeric matrix whose $E'$ is 133 MPa. In fact all the composites have a better performance than matrix alone. This behavior is due to the achieved transference of strength from the fiber to the matrix; this is a consequence of adequate interface and dispersion. In spite of these outstanding results, the other composites do not reach so high a performance in $E'$; for ChS-SB20 the value of $E'$ at 35 °C is 659 MPa, for ChS-SB10 it is 575 MPa and for ChS-SB15 it is 428 MPa. This is caused by the fiber dispersion and non-homogeneity of the natural fibers.

Figure 14 shows the storage modulus ($E'$) for ChS-LB composites. It is possible to observe that these composites do not have a clear tendency with respect to the quantity of reinforcement used. For example, composite with 5% (ChS-LB05) has an $E'$ value of 582 MPa, with 10% (ChS-LB10) only 295 MPa were reached, whereas 475 and 414 MPa were measured for 15% and 20% respectively. In all cases the chitosan-starch matrix ($E'$ = 133 MPa) was surpassed, from the initial temperature and over the test range temperature.

**Figure 13.** Storage modulus (*E'*) for composites (ChS-SB), with 5%–20% of keratin biofiber included.

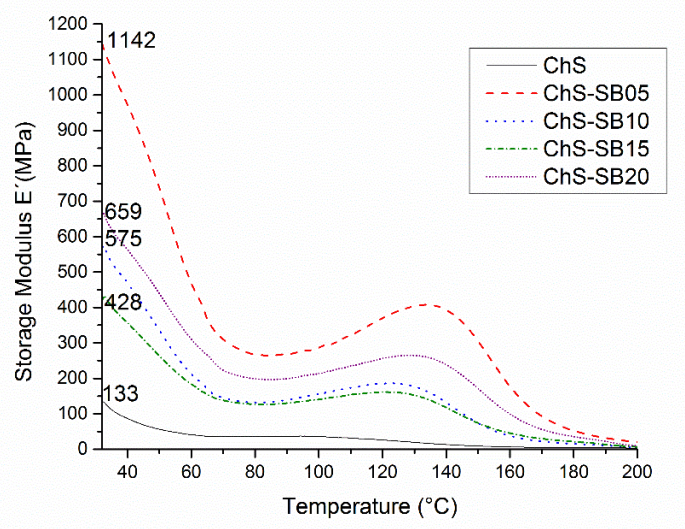


**Figure 14.** Storage modulus (*E'*) for composites (ChS-LB), with 5%–20% of keratin biofiber included.

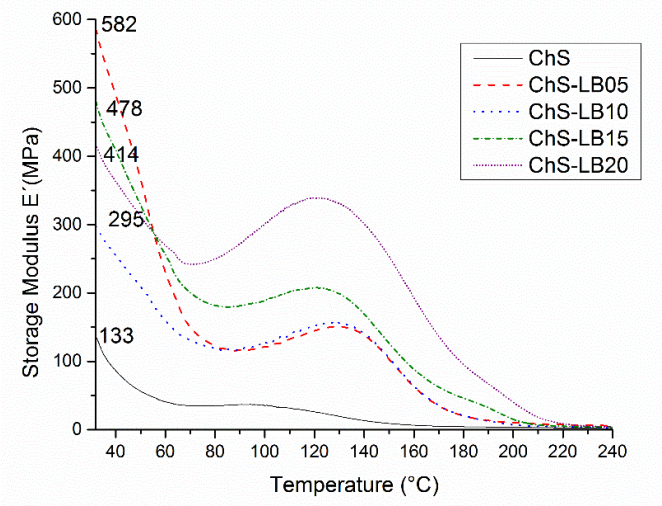


The storage moduli for ChS-GQ composites are shown in Figure 15. These composites have higher *E'* values than the chitosan-starch matrix and present certain trends with respect to quantity of reinforcement. *E'* at 35 °C for matrix was 133 MPa, which was increased to 241, 380 and 527 MPa for ground quill reinforced composites with 5%, 10% and 15% respectively. This beneficial tendency is due to the quill particles having high compatibility with matrix, causing good dispersion and interface. However, an excess in reinforcement causes a slight decrease, since composite with 20% only reaches 256 MPa, probably because the matrix is not enough to cover and wet the quill particles completely.

One interesting fact observed in Figures 13–15 is the behavior of composites at higher temperatures. All reinforced composites show a gradual recovery in *E'* after 80 °C, reaching new maximum values and dropping slowly, whereas *E'* for matrix decreases constantly until arriving at 0 MPa. This performance was apparent in all composites, and can be attributed to keratin materials that

promote intermolecular interactions, reinforcing strongly the thermo mechanical characteristics of the chitosan-starch matrix.

**Figure 15.** Storage modulus (*E'*) for composites (ChS-GQ), with 5%–20% of keratin ground quill included.

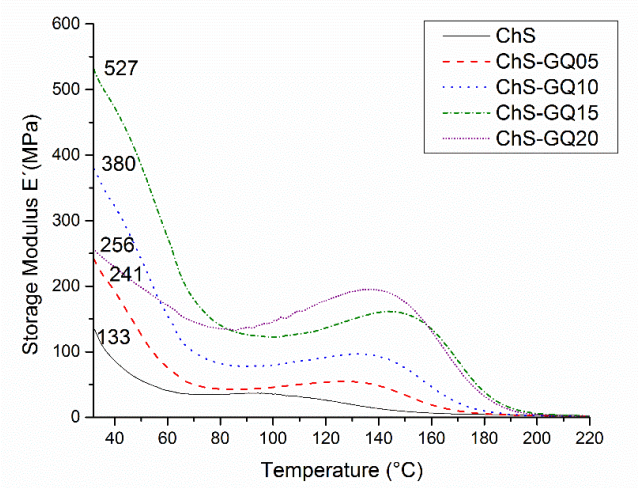


Damping or tan $\delta$ represents the ratio between loss modulus and storage modulus, it depends on the fiber and matrix adhesion, in addition the glass transition temperature ($T_g$) can be deduced from the tan $\delta$ peak [38]. This parameter was evaluated for all composites, the corresponding curves for ChS-SB composites are depicted in Figure 16. There, it is possible to observe that our chitosan-starch matrix has a $T_g$ value in the region near to 126 °C, whereas for ChS-SB composites the values are in the region close to: 164 °C for 5%, 159 °C for 10%, 152 °C for 15% and 166 °C for 20%. This thermal transition peak was shifted to higher temperatures, and at the same time, its intensity was enhanced as the biofiber content was increased. This shift toward higher temperatures can be related to the decreasing mobility of the polymer chain, as a consequence of interaction between fiber and matrix [39].

**Figure 16.** Tan $\delta$ for composites (ChS-SB), with 5%–20% of keratin biofiber included.

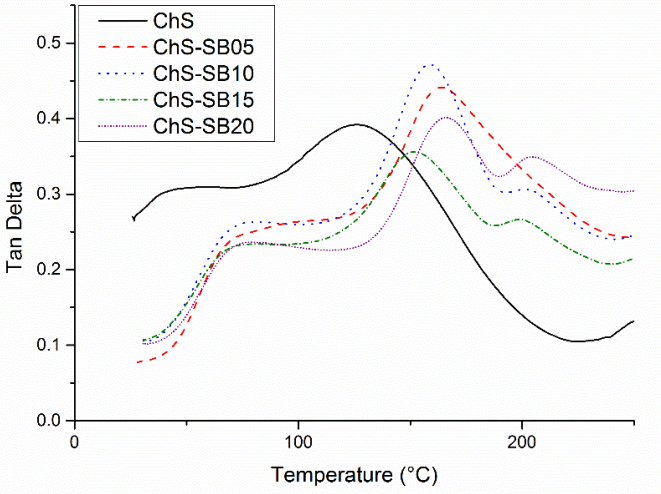

Reinforcement with long keratin biofibers has also a strong influence on the $T_g$ of ChS-LB composites, as can be appreciated in Figure 17. The $T_g$ of the chitosan-matrix was in the region of around 126 °C, while with 5% of reinforcement it was close to 164 °C, with 10% $T_g$ it was increased and appears near to 170 °C, with 15% it was close to 166 °C and with 20% it was adjacent to 185 °C. This change, associated with decreasing mobility of the polymer chain, indicates that long biofibers were able to affect the segmental motions of the biopolymers chains in the chitosan-starch films.

**Figure 17.** Tan $\delta$ for composites (ChS-LB), with 5%–20% of keratin biofiber included.

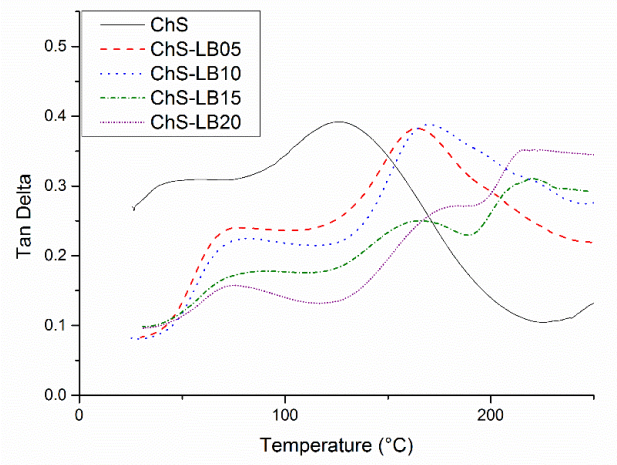


Finally, in Figure 18 it is possible to observe the changes produced by reinforcing with ground quill. ChS-GQ composites have higher $T_g$ values, reaching the region around 159 °C with 5%, close to 178 °C with 10%, in the vicinity of 196 °C with 15% and near 195 °C with 20%. The presence of keratin reinforcement in all cases shows an increase in $T_g$ value, the hydrophobic behavior of keratin fibers [17] produces a decrease in moisture content, thereby reducing the internal friction. Thermal transitions of thermoplastic starch depend on the plasticizer content, the humidity conditions as well as the composition of starch and chitosan [39]. In the same sense chitosan-starch reinforced with keratin biofibers depends on similar parameters.

**Figure 18.** Tan $\delta$ for composites (ChS-GQ), with 5%–20% of keratin biofiber included.

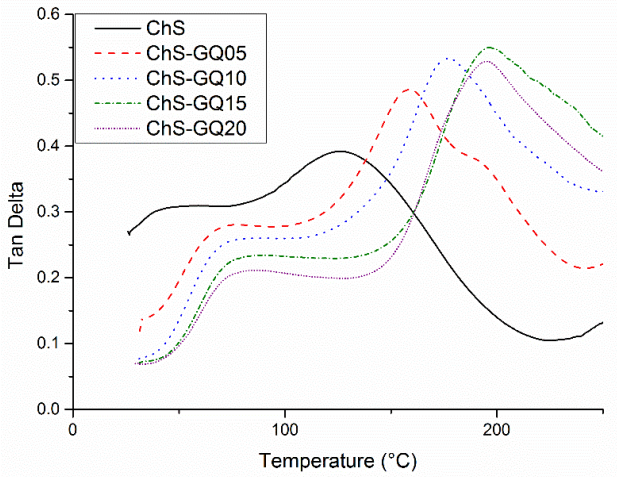

### *3.6. Fourier Transform Infrared Analysis*

FTIR analysis was used to verify the interactions between chitosan, starch and keratin in the composites. Figure 19 shows two regions in the FTIR spectra of chitosan-starch films, keratin and the composites synthesized with 20% (according to Table 1). Figure 19A shows the region from 4000–2500 $cm^{-1}$. In this zone the spectrum related with chitosan starch film **a**) shows the band at 3400 $cm^{-1}$ assigned to the hydrogen-bonded hydroxyl groups due to the presence of starch [40]. In the spectrum **e**) (keratin sample), the main vibrations attributed to the keratin structure were identified in the region around 3300 $cm^{-1}$ and correspond to a range of amide bands, also the peak in 2945 $cm^{-1}$ is assigned to the asymmetric vibration of the CH of the methyl group. The composite films in this region only show broad peaks that are related to the signals of the mentioned peaks, found in chitosan starch films and keratin.

**Figure 19.** IR spectra of the composite films: (**a**) chitosan-starch film (ChS); (**b**) chitosan-starch-short biofiber 20% (ChS-SB20); (**c**) chitosan-starch-long biofiber 20% (ChS-LB20); (**d**) chitosan-starch-ground quill 20% (ChS-GQ20); (**e**) keratin; **A**) from 4000–2500 $cm^{-1}$; **B**) from 1800–700 $cm^{-1}$.

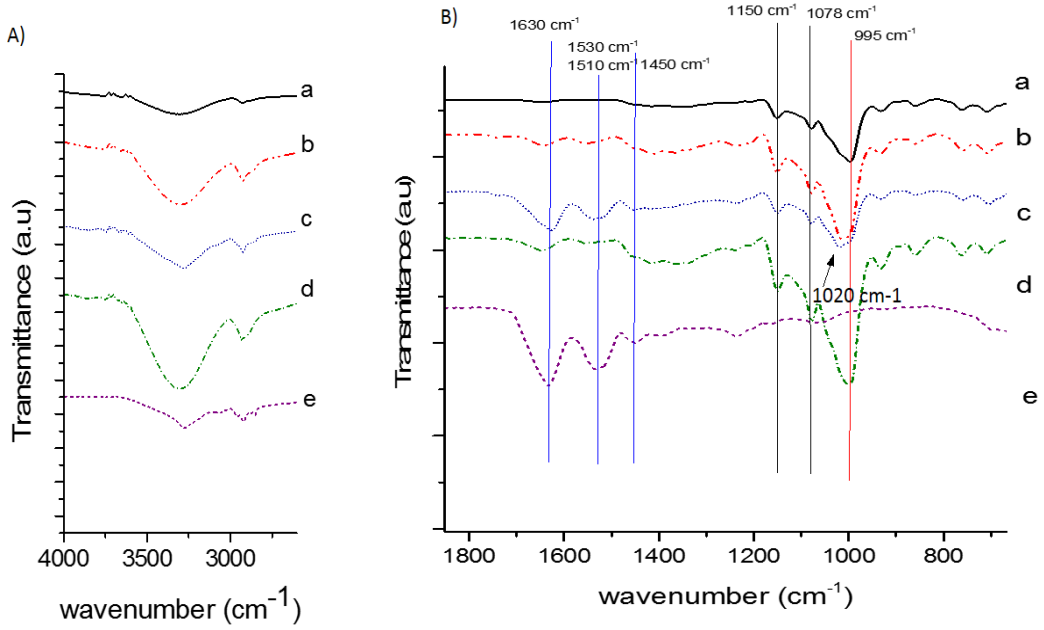


Figure 19B shows the FTIR spectra of chitosan-starch films, keratin and the composites synthesized with 20% (according to Table 1) in the zone from 1800–700 $cm^{-1}$. In this region the main peaks related to chitosan starch films (spectrum a) are detected, the peaks at 700–770 $cm^{-1}$ correspond to the saccharide structure [11], and the three characteristic peaks between 995–1150 $cm^{-1}$ are attributed to C–O bond stretching [40–42]. These peaks are used as references in the composite films, because these bands appear at the same wavenumber than the peaks found in the chitosan- starch spectrum. However, a clear shoulder is found at 1020 $cm^{-1}$ in the spectra of short and large fibers of keratin. This band has been found to be sensitive to interactions of C–O–C in chitosan starch films with hydrogen bonds [41,43]. Results are related to the thermo mechanical properties and the morphological features of the

composite, as a better storage modulus is reached in the composites with short and large fibers than the composite with ground quill. Also better distribution is obtained in these composites.

In the same Figure 19B, the main bands related to keratin are also observed, the band at 1630 $cm^{-1}$ is assigned to the C=O group and the peaks at 1530 $cm^{-1}$ and 1510 $cm^{-1}$ attributed to in plane bending of NH group, while the signal at 1,430 $cm^{-1}$ is related to bending of the $CH_3$ group [1,17,19]. It is possible to observe that these peaks are found in the composite films, but only slight changes are found in the ground quill composite. It is possible that due to the grind, the quill undergoes certain changes in its structure and these bands are sensitive to keratin arrangements in the feathers [17]. Keratin materials stay without detectable changes in the composites.

## 4. Conclusions

Keratin reinforcements, as quill or biofibers, have good compatibility with chitosan-starch matrix, and therefore produce strong interactions that are reflected in the excellent thermal and thermomechanical analyses. The storage modulus of all composites is significantly higher than the chitosan-starch matrix as a result of keratin reinforcement. Thus, the contributions to the matrix properties were found in this order: SB > LB > GQ, from the highest to the lowest. TGA analysis reveals also better thermal stability of composites with respect to the matrix. DSC studies showed changes in endothermic peaks corresponding to water evaporation in all the composites; it is also possible to observe the influence of the crystalline melting temperature of keratin and its decomposition signal. The images of composites and the SEM micrographs show the good distribution of fibers achieved, as well as noted interactions next to the interface. In the FTIR spectra some possible interactions are detected in the C–O bonds. It is worthy of mention that these interactions were accomplished without any superficial treatment to the fiber, that is without any coupling agent. The promising results shown by these materials enable continuity of this research line and as a consequence additional exploration of biodegradation performance and different semi-industrial processes is actually underway, in order to take into account the excellent characteristics of both natural components: matrix and reinforcement. These results are the first study published that incorporates keratin biofibers in a natural matrix composed of chitosan and starch, which is itself an important contribution to eco-composites supported by natural resources.

## Acknowledgments

The authors are grateful to Alicia del Real López for her technical assistance in SEM micrographs. Financial support from CONACyT, as Ph.D. Scholarship, is gratefully acknowledged by Flores-Hernández. Martínez-Hernández and Velasco-Santos also express thanks for the economic support provided by DGEST and Technological Institute of Queretaro through the projects 2499.09-P and QRO-IMA-2012-103, respectively.

## Conflicts of Interest

The authors declare no conflict of interest.

## References


1. Meyers, M.A.; Chen, P.Y.; Lin, A.Y.M.; Seki, Y. Biological materials: Structure and mechanical properties. *Prog. Mater. Sci.* **2008**, *53*, 1–206.
2. Faruk, O.; Bledzki, A.K.; Fink, H.P.; Sain, M. Biocomposites reinforced with natural fibers: 2000–2010. *Prog. Polym. Sci.* **2012**, *37*, 1552–1596.
3. Koronis, G.; Silva, A.; Fontul, M. Green composites: A review of adequate materials for automotive applications. *Compos. B Eng.* **2013**, *44*, 120–127.
4. Brostow, W.; Datashvili, T.; Miller, H.; Wood and wood derived materials. *J. Mater. Educ.* **2010**, *32*, 125–138.
5. Tang, X.Z.; Kumar, P.; Alavi, S.; Sandeep, K.P. Recent advances in biopolymers and biopolymer-based nanocomposites for food packaging materials. *Crit. Rev. Food Sci. Nutr.* **2012**, *52*, 426–442.
6. Espíndola-González, A.; Martínez-Hernández, A.L.; Fernández-Escobar, F.; Castaño, V.M.; Brostow, W.; Datashvili, T.; Velasco-Santos, C. Natural-Synthetic hybrid polymers developed via electrospinning: the effect of PET in chitosan/starch system. *Int. J. Mol. Sci.* **2011**, *12*, 1908–1920.
7. Bustos-Ramírez, K.; Martínez-Hernández, A.L.; Martínez-Barrera, G.; de Icaza, M.; Castaño, V.M.; Velasco-Santos, C. Covalently bonded chitosan on grapheme oxide via redox reaction. *Materials* **2013**, *6*, 911–926.
8. Shukla, S.K.; Mishra, A.K.; Arotiba, O.A.; Mamba, B.B. Chitosan-based nanomaterials: A state-of-the-art review. *Int. J. Biol. Macromol.* **2013**, *59*, 46–58.
9. Xie, F.; Pollet, E.; Halley, P.J.; Avérous, L. Starch-based nano-biocomposites. *Prog. Polym. Sci.* **2013**, *38*, 1590–1628.
10. Cerclé, C.; Sarazin, P.; Favis, B.D. High performance polyethylene/thermoplastic starch blends through controlled emulsification phenomena. *Carbohydr. Polym.* **2013**, *92*, 138–148.
11. Aguilar-Palazuelos, E.; Zazueta-Morales, J.J.; Jiménez-Arevalo, O.A.; Martínez-Bustos, F. Mechanical and structural properties of expanded extrudates produced from blends of native starches and natural fibers of henequen and coconut. *Starch* **2007**, *59*, 533–542.
12. Willett, J.L.; Schrogen, R.L. Processing and properties of extruded starch/polymer foams. *Polymer* **2002**, *43*, 5935–5947.
13. Hang, A.T.; Tae, B.; Park, J.S. Non-woven mats of poly(vinyl alcohol)/chitosan blends containing silver nanoparticles: fabrication and characterization. *Carbohydr. Polym.* **2010**, *82*, 472–479.
14. Bonilla, J.; Fortunati, E.; Vargas, M.; Chiralt, A.; Kenny, J.M. Effects of chitosan on the physochemical and antimicrobial properties of PLA films. *J. Food Eng.* **2013**, *119*, 236–243.
15. Mathew, S.; Brahmakumar, M.; Emilia Abraham, T. Microstructural imaging and characterization of the mechanical, chemical, thermal, and swelling properties of starch-chitosan blend films. *Biopolymers* **2006**, *82*, 176–187.
16. Bourtoom, T.; Chinnan, M.S. Preparation and properties of rice starch-chitosan blend biodegradable film. *Food Sci. Technol.* **2008**, *41*, 1633–1641.
17. Martínez-Hernández, A.L.; Velasco-Santos, C.; de Icaza, M.; Castaño, V.M. Microstructural characterization of keratin fibres from chicken feathers. *Int. J. Environ. Pollut.* **2005**, *23*, 162–178.

18. Martínez-Hernández, A.L.; Velasco-Santos, C. Keratin Fibers from Chicken Feathers: Structure and Advances in Polymer Composites. In *Keratin: Structure, Properties and Applications*; Dullart, R., Mousques, J., Eds.; Nova Science Publishers, Inc.: Hauppauge, NY, USA, 2011; pp.149–211.
19. Martínez-Hernández, A.L.; Velasco-Santos, C.; de Icaza, M.; Castaño, V.M. Grafting of methyl methacrylate onto natural keratin. *e-Polymers* **2003**, *3*, 209–219.
20. Martínez-Hernández, A.L.; Santiago-Valtierra, A.L.; Alvarez-Ponce, M.J. Chemical modification of keratin biofibres by graft polimerization of methyl methacrylate using redox initiation. *Mater. Res. Innov.* **2008**, *12*, 184–191.
21. Rivera-Armenta, J.L.; Flores-Hernández, C.F.; Del Angel-Aldana, R.Z.; Mendoza-Martínez, A.M.; Velasco-Santos, C.; Martínez-Hernández, A.L. Evaluation of graft copolymerization of acrylic monomers onto natural polymers by means infrared spectroscopy. In *Infrared Spectroscopy-Material Science, Engineering and Technology*; Theophanides T., Ed.; InTech: Rijeka, Croatia, 2012; pp. 245–260.
22. Barone, J.R.; Schmidt, W.F.; Liebner, C.F.E. Compounding and molding of polyethylene composites reinforced with keratin feather fiber. *Compos. Sci. Technol.* **2005**, *65*, 683–692.
23. Barone, J.R.; Schmidt, W.F. Polyethelene reinforced with keratin fibers obtained from chicken feathers. *Compos. Sci. Technol.* **2005**, *65*, 173–181.
24. Huda, S.; Yang, Y. Composites from ground chicken quill and polypropylene. *Compos. Sci. Technol.* **2008**, *68*, 790–798.
25. Bullions, T.A.; Hoffman, D.; Gillespie, R.A.; Price-O´Brien, J.; Loos, A.C. Contributions of feather fibers and various cellulose fibers to the mechanical properties of polypropylene matrix composites. *Compos. Sci. Technol.* **2006**, *66*, 102–114.
26. Jiménez-Cervantes Amieva, E.; Velasco-Santos, C.; Martínez-Hernández, A.L.; Rivera-Armenta, J.L.; Mendoza-Martínez, A.M.; Castaño, V.M. Composites from chicken feather quill and recycled polypropylene. *J. Compos. Mater.* **2014**, in press.
27. Martínez-Hernández, A.L.; Velasco-Santos, C.; de Icaza, M.; Castaño, V.M. Mechanical properties evaluation of new composites with protein biofibers reinforcing poly (methyl methacylate). *Polymer* **2005**, *46*, 8233–8238.
28. Saucedo-Rivalcoba, V.; Martínez-Hernández, A.L.; Martínez-Barrera, G.; Velasco-Santos, C.; Castaño, V.M. (Chicken feathers keratin)/polyurethane membranes. *Appl. Phys. A* **2011**, *104*, 219–228.
29. Winandy, J.E.; Muehl, J.H.; Micaels, J.A.; Raina, A. Potential of chicken feather fibre in Wood mdf composites. Available online: http://www.fpl.fs.fed.us/documnts/pdf2003/winan03d.pdf (accessed on 4 March 2014).
30. Hong, C.K.; Wool, R.P. Development of a bio-based composite material from soybean oil and keratin fibers. *J. Appl. Polym. Sci.* **2005**, *95*, 1524–1538.
31. Cheng, S.; Lau, K.; Liu, T.; Yongqing, Z.; Lam, P.; Yin, Y. Mechanical and thermal properties of chicken feather fiber/PLA green composites. *Compos. B* **2009**, *40*, 650–654.
32. Gassner, G.; Line, M.J.; Schmidt, W.; Clayton, T.; Waters, R. Fiber and fiber products produced from feathers. US Patent US5705030, 6 January 1998.

33. Wan, Y.; Lu, X.; Dalai, S.; Zhang, J. Thermophysical properties of polycaprolactone/chitosan blend membranes. *Thermochim. Acta* **2009**, *487*, 33–38.
34. Popescu, C.; Augustin, P. Effect of chlorination treatment on the thermogravimetric behavior of wool fibers. *J. Therm. Anal. Calorim.* **1999**, *57*, 509–515.
35. Balaji, S.; Kumar, R.; Sripriya, R.; Kakkar, P.; Vijaya Ramesh, D. Preparation and comparative characterization of keratin-chitosan and keratin-gelatin composite scaffolds for tissue engineering applications. *Mater. Sci. Eng. C* **2012**, *32*, 975–982.
36. Brostow, W.; Hagg Lobland, H.E.; Narkis, M. Sliding wear, viscoelasticity and brittleness of polymers. *J. Mater. Res.* **2006**, *21*, 2422–2428.
37. Brostow, W.; Hagg Lobland, H.E.; Narkis, M. The concept of materials brittleness and its applications. *Polym. Bull.* **2011**, *67*, 1697–1707.
38. Menard, K.P. *Dynamic Mechanical Analysis: A Practical Introduction*; CRC Press: Boca Raton, FL, USA, 1999.
39. Kaushik, A.; Singh, M.; Verma, G. Green nanocomposites based in thermoplastic starch and steam exploded cellulose nanofibrils from wheat Straw. *Carbohydr. Polym.* **2010**, *82*, 337–345.
40. Mathew, S.; Abraham, T.E. Characterisation of ferulic acid incorporated starch chitosan blend films. *Food Hydrocoll.* **2008**, *22*, 826–835.
41. Akter, N.; Khan, R.A.; Tuhin, M.O.; Haque, M.E.; Nurnabi, M.; Parvin, F.; Islam, R. Thermomechanical, barrier, and morphological properties of chitosan-reinforced starch-based biodegradable composite films. *J. Thermoplast. Compos. Mater.* **2012**, doi:10.1177/0892705712461512.
42. Shen, X.L.; Wu, J.M.; Chen, Y.; Zhao, G. Antimicrobial and physical properties of sweet potato starch films incorporated with potassium sorbate or chitosan. *Food Hydrocoll.* **2010**, *24*, 285–290.
43. Rodríguez-González, C.; Martínez-Hernández, A.L.; Castaño, V.M.; Kharissova, O.V.; Ruoff, R.S.; Velasco-Santos, C. Polysaccharide nanocomposites reinforced with graphene oxide and keratin-grafted graphene oxide. *Ind. Eng. Chem. Res.* **2012**, *51*, 3619–3629.